



ELSEVIER

Available online at www.sciencedirect.com

ScienceDirect

journal homepage: www.elsevier.com/locate/he

Proton incorporation in yttria-stabilized zirconia during atomic layer deposition

Kiho Bae^{a,b}, Kyung Sik Son^a, Jun Woo Kim^a, Suk Won Park^a, Jihwan An^c, Fritz B. Prinz^{c,d}, Joon Hyung Shim^{a,*}

^a School of Mechanical Engineering, Korea University, Anam-dong, Seongbuk-gu, Seoul 136-713, Republic of Korea

^b High-temperature Energy Materials Research Center, Korea Institute of Science and Technology (KIST), Hawolgok-dong, Seongbuk-gu, Seoul 136-791, Republic of Korea

^c Department of Mechanical Engineering, Stanford University, Stanford CA 94305, USA

^d Department of Materials Science and Engineering, Stanford University, Stanford CA 94305, USA

ARTICLE INFO

Article history:

Received 5 September 2013

Received in revised form

6 November 2013

Accepted 11 November 2013

Available online 8 January 2014

Keywords:

Protons

Atomic layer deposition

Yttria-stabilized zirconia

Secondary ion mass spectrometry

ABSTRACT

This work elucidated the proton-incorporation mechanism in ALD YSZ¹. Isotope ²H₂O was used as an oxidant to trace proton incorporation. The ratio of ZrO₂ to Y₂O₃ ALD cycles was varied from 1:1 to 5:1. TEM confirmed that the ALD YSZ films grew as fully crystallized columnar grains in the cubic ZrO₂ phase. SIMS indicated that the Y³⁺ and ²H⁺ concentrations were linearly correlated, indicating yttria-deposition-induced proton incorporation. XPS confirmed an appreciable amount of Y(OH)₃ proportional to the ²H⁺ content in the ALD YSZ, as was also detected by SIMS. Oxide ion vacancies created by the replacement of ZrO₂ with relatively small amounts of Y₂O₃ provided additional vacancies for proton incorporation, resulting in steeper [²H⁺]/[Y³⁺] slopes.

Copyright © 2013, Hydrogen Energy Publications, LLC. Published by Elsevier Ltd. All rights reserved.

1. Introduction

The presence of protons in yttria-stabilized zirconia (YSZ) has been reported by various researchers since the 1960s. The higher mobility of protons in YSZ as compared to that of oxide ions may help reduce the energy loss due to ohmic resistance across electrolyte membranes, and this characteristic has attracted the attention of scientists aiming to develop high-performance electrochemical systems including fuel cells, batteries, gas separators, and sensors [1]. Wagner et al. first reported the reasonably fast diffusion of protons through YSZ at high temperatures and proposed the use of YSZ as an

electrolyte in hydrogen sensors [2,3]. Fast diffusion of protons through nanocrystalline YSZ has recently been reported, and a decrease in grain size has been demonstrated to result in enhanced ionic conductivity [4–9]. It has also been claimed that the incorporation of water into the oxide ion vacancies and the protons orbiting the neutral oxide ions in vacant lattice spaces are responsible for the presence of protons in YSZ. This mechanism is similar to the H⁺ incorporation in doped perovskites with the general formula ABO₃ [10–12]. Oxygen vacancies are particularly likely to be found on the grain surface or along the grain boundaries in doped or undoped ZrO₂ [13]. These claims have led researchers to the conclusion that most protons reside in the inter-granular space as

* Corresponding author. Tel.: +82 2 3290 3353; fax: +82 2 926 9290.

E-mail address: shimm@korea.ac.kr (J.H. Shim).

0360-3199/\$ – see front matter Copyright © 2013, Hydrogen Energy Publications, LLC. Published by Elsevier Ltd. All rights reserved.

<http://dx.doi.org/10.1016/j.ijhydene.2013.11.023>

Nomenclature

$^2\text{H}^+$	deuterium or heavy hydrogen ion
$^2\text{H}_2\text{O}$	water in which deuterium is substituted for hydrogen
$\text{V}_\text{O}^\bullet$	oxide ion vacancy
[M]	molar concentration of ion M

Abbreviations

ALD	atomic layer deposition
YSZ	yttria stabilized zirconia
ALD YSZ	yttria stabilized zirconia film synthesized by atomic layer deposition
CVD	chemical vapor deposition
PLD	pulsed laser deposition
SIMS	secondary ion mass spectrometry
TMA	trimethyl aluminum
TEM	transmission electron microscopy
XPS	X-ray photoelectron spectroscopy

hydroxyl ions, and this conclusion has been supported by extensive experimental evidence [5,6,8,9,12,14,15]. Sakai et al. observed that fewer hydrogen isotope ions ($^2\text{H}^+$) were absorbed into 8 mol% single-crystal YSZ than onto polycrystalline YSZ at the same doping rate when annealing was performed in a $^2\text{H}_2\text{O}$ environment. Therefore, they concluded that most protons in polycrystalline YSZ existed at the grain boundaries [14]. Kim et al. demonstrated that water-incorporated solid oxide fuel cells with nanogranular 8 mol% YSZ could operate successfully at room temperature, whereas similar fuel cells that used microgranular YSZ generated almost no current with the same experimental setup [5]. They also used $^2\text{H}_2\text{O}$ to demonstrate the diffusion of protons through the YSZ electrolyte during fuel cell operation.

Atomic layer deposition (ALD) is a modified chemical vapor deposition (CVD) technique in which films are synthesized one atomic layer at a time by exposing alternating precursors. ALD YSZ films are synthesized by alternating ZrO_2 and Y_2O_3 ALD cycles, and the concentration of the dopant (Y_2O_3) can be adjusted by varying the numbers of ZrO_2 and Y_2O_3 cycles [12,16–21]. The performance of fuel cells employing nanoscale ALD YSZ electrolytes is superior to that of similar fuel cells employing YSZ fabricated using other techniques, exhibiting a power output of 0.28–1.34 W/cm^2 at 265–500 °C [17,20,21]. This is because the concentration of Y_2O_3 plays an important role in determining the ionic properties of YSZ, because the dopant cations (Y^{3+}) replace the host cations (Zr^{4+}) in the zirconia lattice to create empty oxygen sites or oxygen vacancies ($\text{V}_\text{O}^\bullet$) [21]. In the same context, controlling the number of Y_2O_3 cycles is important in ALD, as has been experimentally proven in our previous studies [18,20]. We also observed an abundance of $^2\text{H}^+$ ions in ALD YSZ synthesized using metal-organic precursors and water. These protons are presumed to reside in oxygen vacancies as hydroxyl ions [12]. Interestingly, ALD YSZ allows protons to diffuse more effectively than does YSZ synthesized by pulsed laser deposition (PLD) [12], probably because the former is fabricated in humidified environments [7,12]. Up to now, however, no rigorous study on the relationship between yttria doping and the protonation of

YSZ has been reported. Therefore, in this paper, we have elucidated the mechanism of proton incorporation into ALD YSZ using $^2\text{H}_2\text{O}$ as the source of oxidation during film production. In particular, secondary ion mass spectrometry (SIMS) was used to analyze the concentrations of trace isotopes or $^2\text{H}^+$ in relation to the doping rate.

2. Methodology

2.1. Synthesis and characterization of ALD YSZ

ALD YSZ films were synthesized using a method reported in the literature [17–21]. Tetrakis(dimethylamido)zirconium(IV) and tris(methylcyclopentadienyl)yttrium(III) were used as precursors for the ALD ZrO_2 and Y_2O_3 , respectively. As mentioned above, $^2\text{H}_2\text{O}$ was used as an oxidant. The deposition temperature was set to 250 °C, and the other process parameters and setups were the same as specified in our previous publication [21]. The ratio of ZrO_2 to Y_2O_3 ALD cycles was varied in the range of 1:1–5:1 to fabricate samples called ALD YSZ 1:1–5:1, respectively, and the thickness of the YSZ layers produced was 50 nm. For comparison, pure ZrO_2 was also deposited with $^2\text{H}_2\text{O}$. The ALD YSZ layers prepared with $^2\text{H}_2\text{O}$ were sandwiched between 20 and 30-nm-thick ALD Al_2O_3 layers made from trimethyl aluminum (TMA) and water to prevent the diffusion of $^2\text{H}^+$ ions between the layers or into air upon subsequent exposure to ambient environments. All layers were deposited consecutively without any exposure to air. A schematic structure of the sample is illustrated in Fig. 1. The microstructure and thickness of the films were evaluated using transmission electron microscopy (TEM; JEM 2100F at Korea Basic Science Institute (KBSI)). X-ray photoelectron spectroscopy (XPS; SSI S-Probe, monochromated Al $K\alpha$ radiation at Korea Institute of Science and Technology (KIST)) was performed for compositional analyses.

2.2. Experiments on proton diffusion

To verify that the ALD Al_2O_3 prevented $^2\text{H}^+$ ion diffusion, we fabricated 50-nm-thick Al_2O_3 layers with $^2\text{H}_2\text{O}$ on a Si wafer and carried out in-depth measurements of the concentrations of $^2\text{H}^+$ and other component cations including Al^{3+} , Zr^{4+} , and Y^{3+} using time-of-flight SIMS (TOF-SIMS: ION-TOF at the Korea Institute of Science and Technology (KIST)). The energy of the primary ion beam was set to 25 keV, with a beam current of 1 pA, and the area analyzed was 100 $\mu\text{m} \times 100 \mu\text{m}$.

3. Results and discussion

3.1. Structural characteristics of ALD YSZ

The microstructures of the ALD YSZ 1:1–5:1 and ALD ZrO_2 films were analyzed using cross-sectional TEM images. From this analysis, it was clear that all the ALD YSZ films grew as fully crystallized columnar grains regardless of the Y_2O_3 content, whereas the capping ALD Al_2O_3 layers grew with amorphous structures (Fig. 2). The measured widths of the grains were in the range of 3–20 nm. There was no substantial

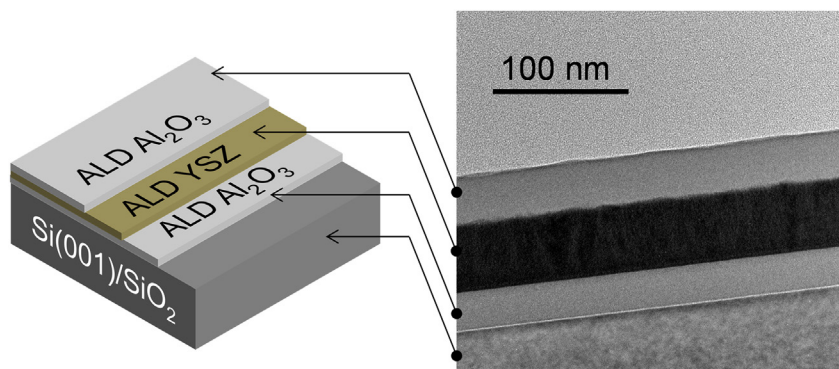


Fig. 1 – Sample setup of the yttria-stabilized zirconia (YSZ) thin films with Al_2O_3 capping layers synthesized by atomic layer deposition (ALD). Each YSZ layer was sandwiched between Al_2O_3 layers to block atomic diffusion from substrate and outer layer.

difference in atomic spacing in any orientation, as confirmed by the high-resolution TEM (HRTEM). There was also no apparent physical space between the columnar grains (Figs. 2 and 3). This phenomenon was also observed in our previous work on ALD YSZ films [21]. The phase of the film was further analyzed using diffraction patterns obtained from the HRTEM images (Fig. 3). For cubic crystals with a lattice constant a , the spacing d between adjacent lattice planes can be calculated as

$$d = \sqrt{a^2 / (h^2 + k^2 + l^2)}$$

where $(h\ k\ l)$ represents a plane normal to a direction (h, k, l) . Accordingly, the d -spacing values can be calculated from the cubic ZrO_2 lattice constant ($a = 5.139\ \text{\AA}$) as 0.2967, 0.2570,

0.1817, and 0.1533 nm for the (111), (200), (220), and (311) orientations, respectively. As shown in the inset tables in Fig. 3, the d -values from all of the ALD YSZ samples and pure ALD ZrO_2 correspond to those calculated from cubic ZrO_2 . Therefore, we can conclude that the ALD YSZ films grow as columnar nanoscale grains and that the grains are fully crystallized in the cubic ZrO_2 phase regardless of the Y_2O_3 doping rate.

3.2. Compositional characteristics of ALD YSZ

In the SIMS profiles (Fig. 4), we found that the concentration of $^2\text{H}^+$ in the ALD Al_2O_3 was substantially lower than that in the

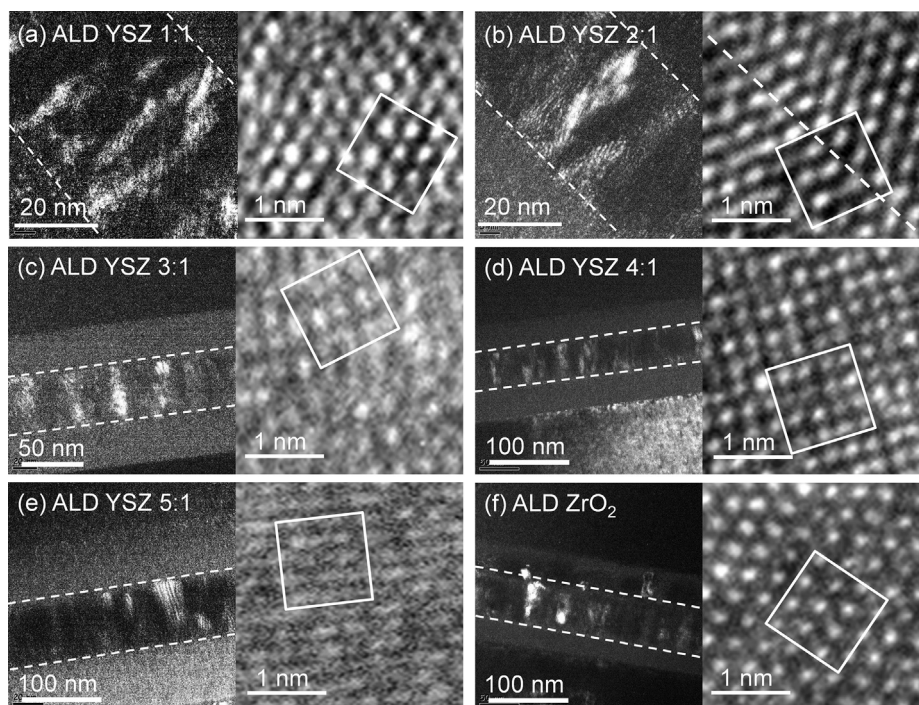


Fig. 2 – High-contrast transmission electron microscopy (TEM) (left) and high-resolution TEM (HRTEM) images (right) of pure ZrO_2 and yttria-stabilized zirconia (YSZ) prepared by atomic layer deposition (ALD) with cycle ratios varying from 1:1 to 5:1 ($\text{ZrO}_2:\text{Y}_2\text{O}_3$). Broken line in HRTEM images indicates grain boundary.

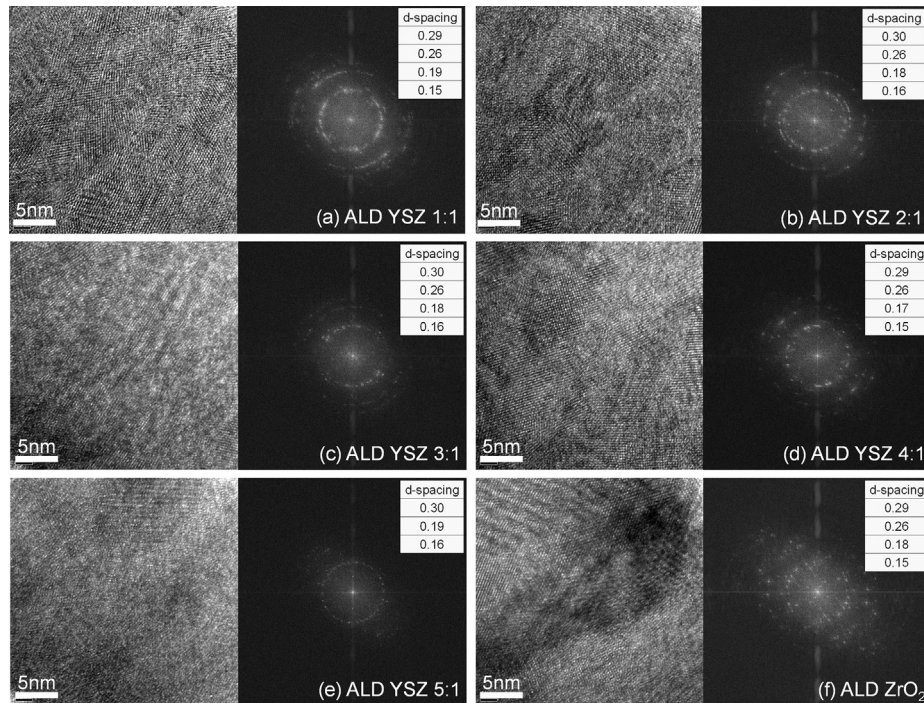


Fig. 3 – High-resolution transmission electron microscopy (HRTEM) images and diffraction patterns of the ZrO_2 and yttria-stabilized zirconia (YSZ) prepared by atomic layer deposition (ALD) with d -spacing measured from diffraction images.

ALD YSZ, which indicates that the protons did not diffuse through or reside in the alumina layer. Therefore, it is confirmed that ALD Al_2O_3 effectively blocked $^2\text{H}^+$ diffusion and that the $^2\text{H}^+$ ions present in the YSZ must have been introduced during the ALD cycles and not before or after

deposition. The concentration of $^2\text{H}^+$ near the interface between the bottom alumina layer and the Si wafer detected at about a sputtering time of 600 s (Fig. 4) was higher than that in Al_2O_3 , presumably because of proton diffusion into the native silicon oxide present at the interface. The sudden spikes/

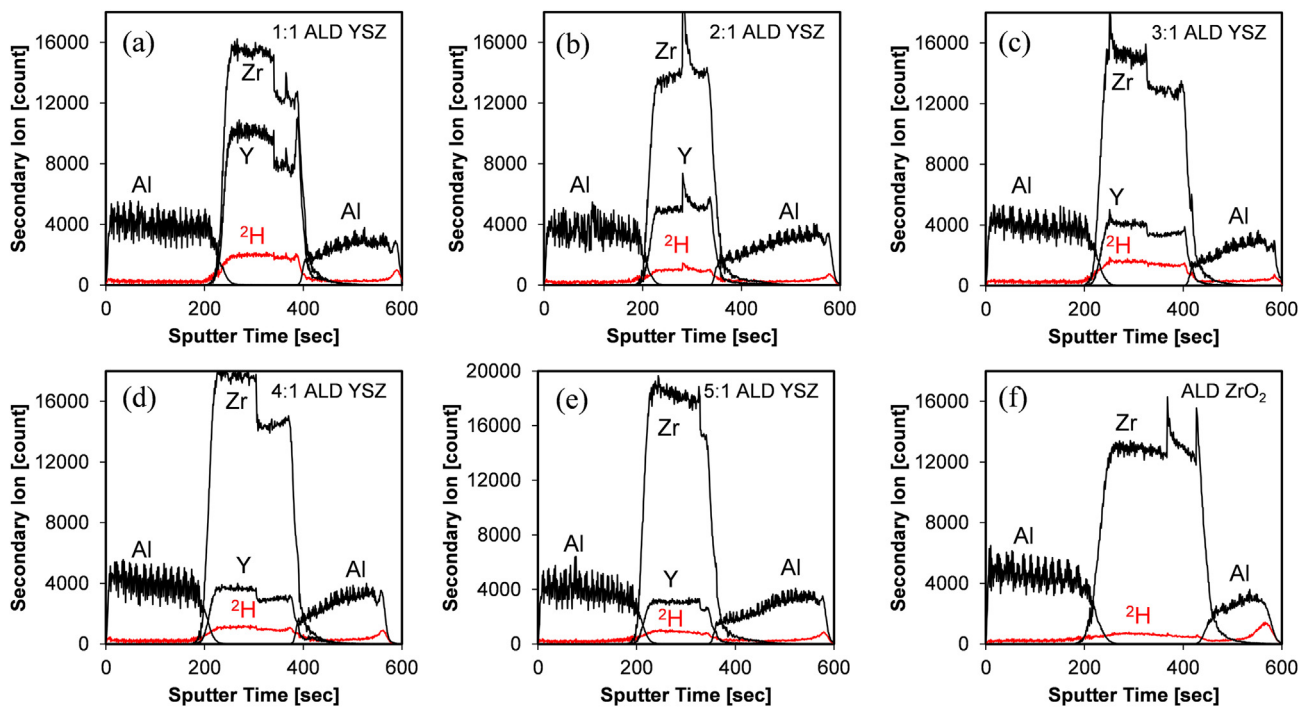


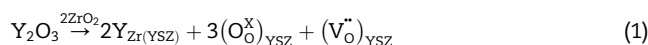
Fig. 4 – Depth profiles of Al^{3+} , Zr^{4+} , Y^{3+} , and $^2\text{H}^+$ concentrations in pure ZrO_2 and yttria-stabilized zirconia (YSZ) prepared by atomic layer deposition (ALD) obtained from time-of-flight secondary ion mass spectrometry (TOF-SIMS).

sharp drops in the composition profiles at about 300 s of sputtering time were the result of the inconsistent sensitivity of the SIMS detector, and the composition changed little through the YSZ layer. More Y^{3+} ions were detected in the samples fabricated with a greater number of ALD Y_2O_3 deposition cycles, as expected.

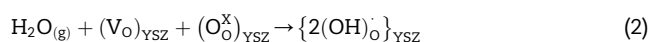
Fig. 5 shows the relationship between the relative concentrations of the ions detected in the ALD YSZ and ZrO_2 layers. Relative concentrations, and not absolute counts, were used in the analysis in order to eliminate artifacts resulting from inconsistent detector sensitivity. Ninety points were used in each plot to allow a fair and valid composition correlation analysis. As observed in the depth profiles (Fig. 4), the concentrations of Y^{3+} and Zr^{4+} ions showed a negative linear correlation in all the ALD YSZ samples, as shown in Fig. 5(a). Fig. 5(c) clearly shows that the relative concentrations of the Y^{3+} and $^2H^+$ ions were linearly correlated in the samples. The ALD YSZ 1:1 and 2:1 profiles fitted well to a linear curve with a slope of 0.1971 and $R^2 = 0.9771$, while the 3:1, 4:1, and 5:1 samples were aligned with a steeper line (slope = 0.5656, $R^2 = 0.8327$). In comparison, the relative Al^{3+} and $^2H^+$ ion contents in ALD Al_2O_3 showed no particular trend in any of the samples (Fig. 5(b)).

There is a greater probability for $Y(OH)_3$ to form from Y_2O_3 during ALD in the presence of water [23], rather than $Zr(OH)_4$, as the latter is difficult to form and the deposition of hydrous zirconia ($ZrO_2 \cdot nH_2O$) is preferred [24]. Therefore, we can infer that the Y^{3+} ions caused chemisorption of water during deposition, which resulted in the formation of a proportional number of hydroxide ions or protons in ALD YSZ, as observed in the SIMS profiles. Niinistö and coworkers reported that ALD Y_2O_3 synthesized with tris(methylcyclopentadienyl) yttrium (III) and water, as done by us, contains a substantial amount of hydrogen impurities and stated that the $[Y^{3+}]/[O^{2-}]$ ratio increased as the H^+ concentration decreased [25]. We believe that the H impurities observed in their experiments could have also originated from $Y(OH)_3$. In their work, the $[Y^{3+}]/[O^{2-}]$ ratio in the film deposited at 200 °C was 0.65, which is slightly smaller than the stoichiometric value of 0.67, when the H^+ concentration was 6.8%. Assuming that the ALD film was a combination of Y_2O_3 and $Y(OH)_3$, the corresponding ratio of Y_2O_3 and $Y(OH)_3$ must be about 97.7:2.3, where $[Y^{3+}]/[O^{2-}]$ is about 0.652, which perfectly matches the measured data. In

addition, the use of water vapor as an oxidizing agent at a relatively low temperature (250 °C), which is an intrinsic characteristic of the film fabrication process, may have been favorable for the formation of hydroxide compounds in the material, as discussed in our previous work [12]. XPS measurements confirmed that the $Y(OH)_3$ content is relatively high in samples ALD YSZ 1:1 and 3:1 and the lowest in the 5:1 sample, as shown in Fig. 6 and Table 1. This trend coincides with that identified in the $^2H^+$ concentration profiles measured by SIMS (Table 1). Interestingly, plots of the relative concentrations of $^2H^+$ versus Y^{3+} for the samples with low Y^{3+} contents (ALD YSZ 3:1, 4:1, and 5:1) could be fitted to a line steeper than that in similar plots for samples with high Y^{3+} contents (ALD YSZ 1:1 and 2:1). We believe that this difference is due to the presence of additional oxide ion vacancies for proton incorporation in the samples with little Y^{3+} , in addition to the hydroxyl ions in $Y(OH)_3$. When ZrO_2 is mixed with relatively smaller amounts of Y_2O_3 , the Zr^{4+} cations are replaced with Y^{3+} ions in the ZrO_2 host structure to create vacancies according to the following process:



Here, V_{O}^{\bullet} represents an oxide ion vacancy and O_{O}^{\times} represents neutral oxygen. In a humid environment, water tends to be chemisorbed at the vacancies and dissociates into hydroxyl groups. This process can be expressed by the following reaction:



where $(OH)_{O}^{\cdot}$ represents the protonic defect associated with lattice oxygen [25]. However, this vacancy formation reaction becomes less favorable in the presence of relatively large amounts of Y_2O_3 , which prefers to form a composite cermet with ZrO_2 . We believe that this results in fewer $^2H^+$ ions being incorporated per Y^{3+} , as can be seen from the smaller $[^2H^+]/[Y^{3+}]$ slope in the SIMS profiles of samples ALD YSZ 1:1 and 2:1.

4. Conclusions

To elucidate mechanism of proton incorporation in ALD YSZ, the water isotope 2H_2O was used as an oxidant so that the

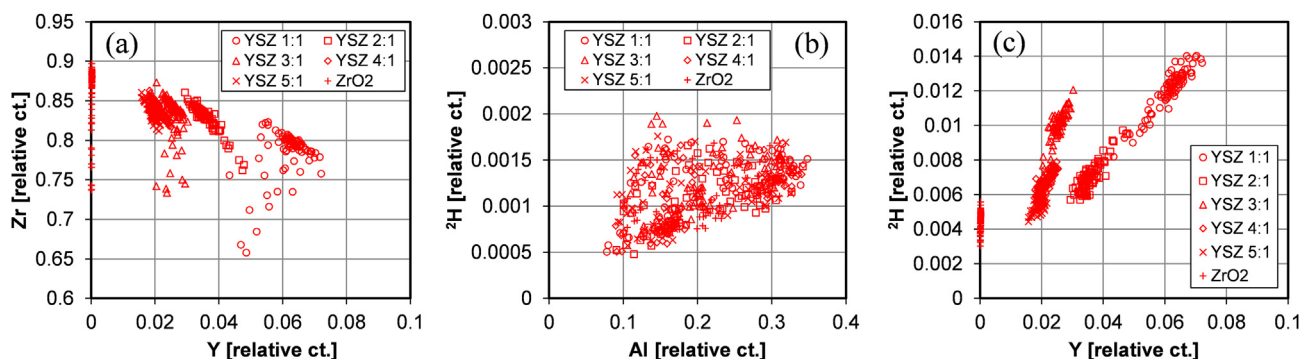


Fig. 5 – Relationship between cation contents in pure ZrO_2 and yttria-stabilized zirconia (YSZ) prepared by atomic layer deposition (ALD), measured by time-of-flight secondary ion mass spectrometry (TOF-SIMS) depth profiling: (a) relative counts of Zr^{4+} versus Y^{3+} in ALD YSZ layers, (b) $^2H^+$ versus Al^{3+} in Al_2O_3 layers, and (c) $^2H^+$ versus Y^{3+} in ALD YSZ layers.

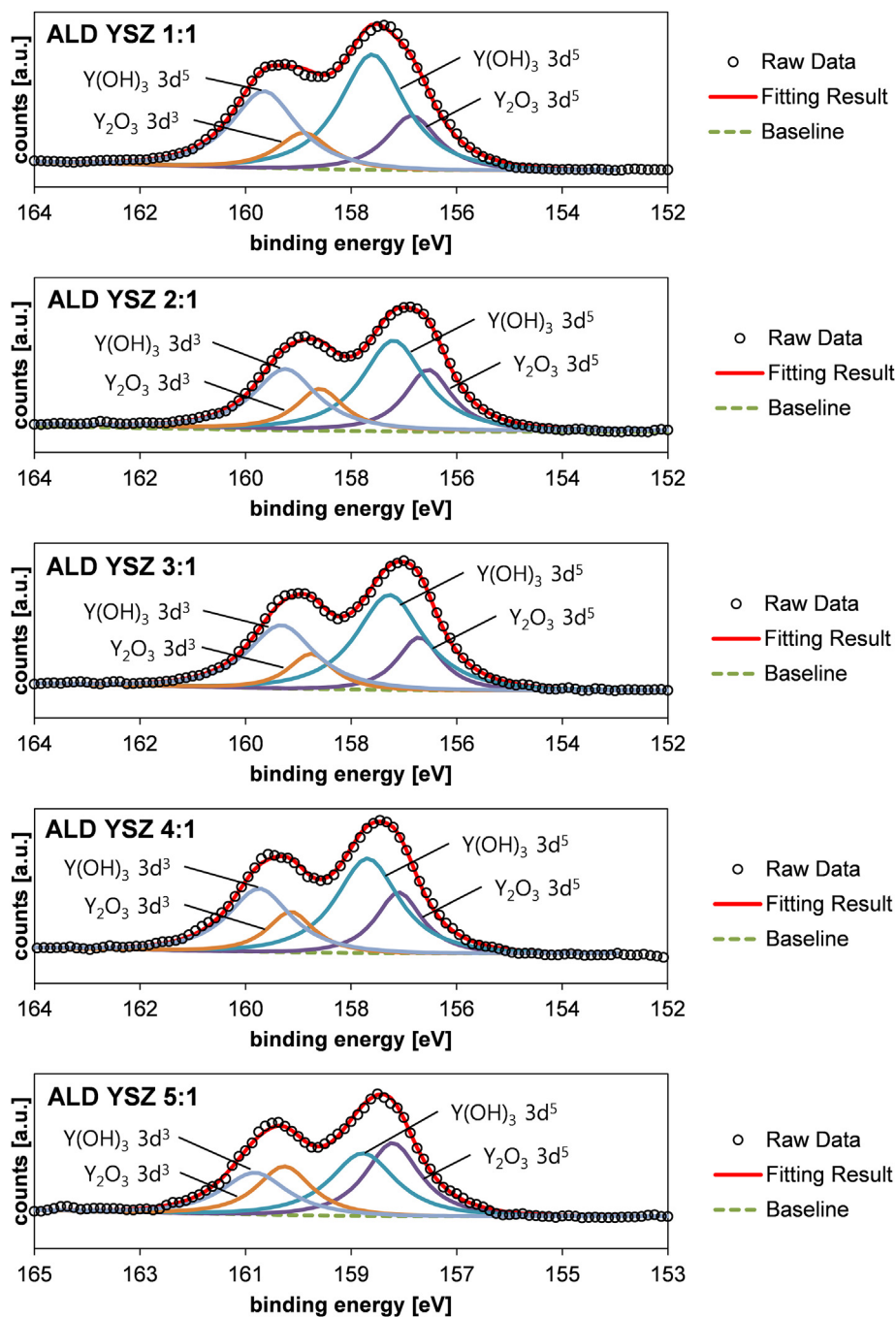


Fig. 6 – X-ray photoelectron spectroscopy (XPS) $Y3d$ spectra of yttria-stabilized zirconia (YSZ) prepared by atomic layer deposition (ALD) after surface etching, fitted to standard $Y(OH)_3$ and Y_2O_3 XPS profiles.

proton incorporation could be traced. To exclude the diffusion of protons or water into the films from the substrates or the external environment after deposition, the prepared films were sandwiched between 20 and 30-nm-thick ALD Al_2O_3 block layers. We prepared ALD films of pure ZrO_2 and films deposited with $ZrO_2 \cdot Y_2O_3$ ALD cycle ratios in the range of 1:1–5:1. The TEM images confirmed that ALD ZrO_2 and ALD YSZ grew as fully crystallized columnar grains with widths of 3–20 nm with no apparent physical space between them. The ALD YSZ films were deposited in the cubic ZrO_2 phase regardless of the Y_2O_3 doping rate. TOF-SIMS was used to

measure the depth profiles of the concentrations of Al^{3+} , Zr^{4+} , Y^{3+} , and $^2H^+$ ions. The SIMS measurement confirmed that the Y^{3+} and $^2H^+$ ion contents were linearly correlated in the ALD samples. It was found that the $^2H^+$ concentration is relatively high in samples ALD YSZ 1:1 and 3:1 and the lowest in the 5:1 sample. This trend also coincides with the $Y(OH)_3$ content confirmed by the XPS spectra. This implies that the Y^{3+} ions caused chemisorption of water during deposition, which in turn resulted in the formation of $Y(OH)_3$ in the ALD YSZ. The $[^2H^+]/[Y^{3+}]$ slope was smaller in samples ALD YSZ 1:1 and 2:1 than in the 3:1–5:1 samples, suggesting that oxide ion

Table 1 – Y(OH)₃ and Y₂O₃ contents estimated by fitting X-ray photoelectron spectroscopy (XPS) Y3d spectra and average relative counts of ²H⁺ ions measured by secondary ion mass spectrometry (SIMS) in the yttria-stabilized zirconia (YSZ) thin films prepared by atomic layer deposition (ALD).

ZrO ₂ :Y ₂ O ₃ cycle ratio	1:1	2:1	3:1	4:1	5:1
Y3d Y(OH) ₃ (XPS)	72.9%	66.5%	73.1%	68.0%	50.7%
Y3d Y ₂ O ₃ (XPS)	27.1%	33.5%	26.9%	32.0%	49.3%
Y3d Y(OH) ₃ /Y ₂ O ₃ (XPS)	2.69	1.98	2.72	2.13	1.03
Relative avg. ² H ⁺ cts. (SIMS)	1.21%	0.696%	0.911%	0.640%	0.505%

vacancies V_O^{••} were created in addition to the Y(OH)₃, which caused protons to be incorporated when ZrO₂ was replaced with a relatively small amount of Y₂O₃ in the ALD YSZ 3:1–5:1 films.

Acknowledgments

We are grateful to the Fusion Research Program for Green Technologies of the National Research Foundation (NRF) of Korea funded by the Ministry of Education, Science, and Technology (grant no. NRF-2011-0019300).

REFERENCES

- [1] Kreuer KD. Proton-conducting oxides. *Annu Rev Mater Res* 2003;33:333–9.
- [2] Stotz S, Wagner C. The solubility of water vapor and hydrogen in solid oxides. *Ber Bunsenges Phys Chem* 1966;70(8):781–8.
- [3] Wagner C. Solubility of water vapour in ZrO₂–Y₂O₃ solid solutions. *Ber Bunsenges Phys Chem* 1968;72:778–81.
- [4] Anselmi-Tamburini U, Maglia F, Chiodelli G, Riello P, Bucella S, Munir ZA. Enhanced low-temperature protonic conductivity in fully dense nanometric cubic zirconia. *Appl Phys Lett* 2006;89:163116–23.
- [5] Kim S, Anselmi-Tamburini U, Park HJ, Martin M, Munir ZA. Unprecedented room-temperature electrical power generation using nanoscale fluorite-structured oxide electrolytes. *Adv Mater* 2008;20:556–9.
- [6] Chiodelli G, Maglia F, Anselmi-Tamburini U, Munir ZA. Characterization of low temperature protonic conductivity in bulk nanocrystalline fully stabilized zirconia. *Solid State Ionics* 2009;180:297–301.
- [7] Kim S, Avila-Paredes HJ, Wang S, Chen CT, De Souza RA, Martin M, et al. On the conduction pathway for protons in nanocrystalline yttria-stabilized zirconia. *Phys Chem Chem Phys* 2009;11:3035–8.
- [8] Avila-Paredes HJ, Zhao J, Wang S, Pietrowski M, De Souza RA, Reinholdt A, et al. Protonic conductivity of nano-structured yttria-stabilized zirconia: dependence on grain size. *J Mater Chem* 2010;20:990–4.
- [9] Scherrer B, Schlupp MVF, Stender D, Martynczuk J, Grolig JG, Ma H, et al. On proton conductivity in porous and dense yttria stabilized zirconia at low temperature. *Adv Funct Mater* 2012;23:1957–64.
- [10] Guo X. On the degradation of zirconia ceramics during low-temperature annealing in water or water vapor. *J Phys Chem Solids* 1999;60:539–46.
- [11] Guo X. Property degradation of tetragonal zirconia induced by low-temperature defect reaction with water molecules. *Chem Mater* 2004;16:3988–94.
- [12] Park JS, Kim YB, Shim JH, Kang S, Gür TM, Prinz FB. Evidence of proton transport in atomic layer deposited yttria-stabilized zirconia films. *Chem Mater* 2010;22:5366–70.
- [13] Guo X, Zhang Z. Grain size dependent grain boundary defect structure: case of doped zirconia. *Acta Mater* 2003;51:2539–47.
- [14] Sakai N, Yamaji K, Horita T, Kishimoto H, Xiong YP, Yokokawa H. Significant effect of water on surface reaction and related electrochemical properties of mixed conducting oxides. *Solid State Ionics* 2004;175:387–91.
- [15] Raz S, Sasaki K, Maier J, Riess I. Characterization of adsorbed water layers on Y₂O₃-doped ZrO₂. *Solid State Ionics* 2001;143:181–4.
- [16] Putkonen M, Sajavaara T, Niinistö J, Johansson LS, Niinistö L. Deposition of yttria-stabilized zirconia thin films by atomic layer epitaxy from β-diketonate and organometallic precursors. *J Mater Chem* 2002;12:442–8.
- [17] Shim JH, Chao C, Huang H, Prinz FB. Atomic layer deposition of yttria-stabilized zirconia for solid oxide fuel cells. *Chem Mater* 2007;19:3850–4.
- [18] Su PC, Chao C-C, Shim JH, Fasching R, Prinz FB. Solid oxide fuel cell with corrugated thin film electrolyte. *Nano Lett* 2008;8:2289–92.
- [19] Chao C-C, Kim YB, Prinz FB. Surface modification of yttria-stabilized zirconia electrolyte by atomic layer deposition. *Nano Lett* 2009;9:3626–8.
- [20] Chao C-C, Hsu C-M, Cui Y, Prinz FB. Improved solid oxide fuel cell performance with nanostructured electrolytes. *ACS Nano* 2011;5:5692–6.
- [21] Son KS, Bae K, Kim JW, Ha JS, Shim JH. Ion conduction in nanoscale yttria-stabilized zirconia fabricated by atomic layer deposition with various doping rates. *J Vac Sci Technol A* 2013;31. 01A107–01A114.
- [22] Rouffignac P, Park J-S, Gordon RG. Atomic layer deposition of Y₂O₃ thin films from yttrium tris(N,N'-diisopropylacetamidate) and water. *Chem Mater* 2005;17:4808–14.
- [23] Huang C, Tang Z, Zhang Z. Differences between zirconium hydroxide (Zr(OH)₄·nH₂O) and hydrous zirconia (ZrO₂·nH₂O). *J Am Ceram Soc* 2001;84:1637–8.
- [24] Niinistö J, Putkonen M, Niinistö L. Processing of Y₂O₃ thin films by atomic layer deposition from cyclopentadienyl-type compounds and water as precursors. *Chem Mater* 2004;16:2953–8.